Rotational Isomeric State Approach to the Single-Chain Behavior of Aromatic Polyesters

G. C. Rutledge†

Interdisciplinary Research Centre in Polymer Science and Technology and Department of Physics, University of Leeds, Leeds LS2 9JT, U.K.

Received January 8, 1992; Revised Manuscript Received March 27, 1992

ABSTRACT: A statistical mechanics analysis based on rotational isomeric state (RIS) theory is applied to the analysis of single-chain behavior in a family of aromatic polyester compositions, including homopolymers of 1-hydroxy-4-benzoic acid and 6-hydroxy-2-naphthoic acid, their related nonregular copolymers, and a series of nonregular terpolymers containing the *m*-phenylene aromatic moiety. Averages of chain rigidity and shape are determined over all allowed conformations and constitutions of chains of fixed average composition in the long-chain limit. The variety of conformational behaviors exhibited by representatives within this large group of polymers clearly distinguishes the stiff-chain members of the family from those more closely approaching random coil behavior. A variation of the conventional RIS treatment incorporating higher moments of the torsion angle distribution in the assignment of isomeric states for the ester bond dihedral is used to capture the effect of torsion angle fluctuations in long chains of aromatic polyesters without recourse to extensive molecular dynamics simulations. Calculated values of chain persistence length a ranging from ~200 Å down to 20 Å for a variety of compositions are in good agreement with the available experimental data. A distinction may be drawn between the single-chain behavior in dilute solution and that anticipated in the oriented solid state, primarily due to intermolecular packing constraints.

Introduction

Aromatic polyesters, or polyarylates, comprise a group of chemically similar, yet behaviorly diverse polymers, the individual properties of members of which are controlled through selection of monomer composition at synthesis. In most general terms, these polyesters consist entirely of aromatic backbone groups joined, either in regular or in nonregular sequences, by intervening ester linkages. Important members of this family of materials include the copolymers of *p*-hydroxybenzoic acid (HBA) and 6-hydroxy-2-naphthoic acid (HNA), which exhibit thermotropic liquid crystallinity and may be spun into high-performance fibers or melt-phase formed into high-strength parts. A variety of compositions, involving alteration of the monomer content of the polymer either in kind or in concentration, have been considered by both industry and academia in attempts to gain attractive new combinations of structural properties and processing characteristics.

In this work we attempt to place the key conformational features of these materials on a more general footing in order to address questions concerning the impact of composition and processing on solid-state behavior. Of particular interest are the polyesters which contain elements of the following moieties: (I) *p*-phenylene, (II) *m*-phenylene, (III) 2,6-disubstituted naphthylene, and (IV) 4,4′-disubstituted biphenylene. Thus this study addresses in part the full range of materials including (but not necessarily limited to) the homopolymers poly(4-oxy-1-benzoate) (PHBA) and poly(6-oxy-2-naphthoate) (PHNA), regular copolymers such as poly(*p*-phenylene terephthalate) (PPT) and poly(*p*-phenylene isophthalate) (PPI), the full range of compositions of the nonregular copolymers composed of HBA and HNA monomers, and numerous representatives of the various candidates for attractive nonregular terpolymers, such as that composed of HBA, isophthalic acid (IA), and hydroquinone (HQ). The regular polymers are of special interest primarily as model systems for understanding the behavior of the technically more practical nonregular materials. The HBA/HNA copolymers (henceforth abbreviated BN) are commercially viable high-performance structural polymers; the HBA/IA/HQ terpolymers (henceforth abbreviated HIQ) exhibit unusual structural and mechanical properties which suggest that much valuable information content may be gained by their contrast with the more successful copolymers. Materials containing the 4,4′-biphenylene moiety are of interest primarily for their exceptional mechanical properties relative to the other members of the family.

Experimental data on polyarylates relevant to the determination of segmental conformation and orientation arise from several sources: (i) Crystal structure determination[1,2] and crystal/crystal phase transitions[2,3] have been analyzed in homopolymer PHBA and PPT. In the BN polymers, observations of aperiodic meridional maxima in wide-angle X-ray diffraction (WAXD) have been treated in terms of nonregular chain constitution.[4-7] (ii) Molecular conformation and segmental alignment have been studied for several polyarylates using tension/shear coupling in dynamic mechanical tests[8-11] and in particular for a series of BN copolymers using proton spin/spin relaxation measurements in nuclear magnetic resonance (NMR) spectroscopy.[12,13] (iii) Aperiodic "kinks" in the molecular structure, introduced in the form of monomers based on the *m*-phenylene unit, have been introduced in order to determine their influence on structure and phase behavior,[14-16] segment orientation and molecular alignment,[17] WAXD, and mechanical modulus.[18-20] We have also studied a member of this group of *m*-phenylene-based terpolymers by solid-state proton NMR.[21]

The HIQ subgroup in particular is unusual for the diverse behaviors exhibited by its constitutents. The "pure" compositions, PHBA and PPI, show a strong tendency to crystallize. Compositions containing in excess of 60% HBA content (i.e., less than 20% IA) tend to be intractable and decompose at temperatures below their crystal/nematic transition temperatures. Compositions containing 30–60% HBA exhibit crystal/thermotropic nematic transitions below the decomposition temperature, and the compositions composed of HBA/IA/HQ in proportions 2:1:1 and 1:1:1 in particular have been identified

† Current address: Department of Chemical Engineering, Massachusetts Institute of Technology, Cambridge, MA 02139.

0024-9297/92/2225-3984$03.00/0

as spinnable compositions. The polymers containing less than 30% HBA exhibit only crystal/isotropic melt transitions or are at best borderline cases for thermotropic liquid crystal polymers.

In this work we set out to elucidate the molecular basis for the determination of chain geometry, orientation, and ultimately intermolecular packing as a function of chemical composition. Due to the introduction of two, three, or more monomer types into the chain, often in an essentially random manner (limited only by the requirements of chemical connectivity in the form of ester linkages), the range of constitutions encompassed within the scope of this analysis comprises a very large number of chemical architectures of varying composition, monomer sequence, and monomer conformation. We take a statistical mechanical approach to characterize chain rigidity and molecular "shape" as functions of chemical composition across the spectrum of polyarylate compositions. We also consider two aspects of particular importance to understanding thermotropic liquid crystalline polymer behavior: the torsional flexibility resulting from thermally enhanced fluctuation of bond dihedrals about their average values, and intermolecular packing forces which serve to alter the distribution of conformation states.

Model Construction

Description of the Polyester Chain. All of the materials evaluated within the context of this method consist of alternating backbone mesogens and ester linkages and fit within a relatively simple framework. In this case, the mesogens are, without exception, aromatic groups; one may, with only minor modification, introduce alkane segments between ester linkages. Each aromatic group is bifunctional; in the polyesters, these functional groups are hydroxyl and carboxylic acid groups. Thus we define a pool of available monomers, each consisting of the general formula X–R–Y, where R denotes the ring group identity and X and Y identify the monomer's functional groups, either O or C(O). In cases where the monomer is asymmetric, due either to asymmetry of the ring group or to asymmetric functionalization of the monomer, we distinguish between two related monomers, the head/tail orientation and its tail/head analogue. From the four aromatic moieties mentioned above (I–IV), 16 possible monomers are defined, each aromatic group being combined with one of four sets of ester-forming linkage groups of either the type X–R–X, where X represents either (i) the ester oxygen (diol monomer) or (ii) the ester carbonyl (diacid monomer), or type X–R–Y, where X and Y differ, representing the two orientations of the asymmetric acid/alcohol monomer.

The calculation of conformation averages of the persistence vector, mean squared end-to-end distance, or radius of gyration for any specified sequence of monomers up to a predetermined degree of polymerization may be accomplished by conventional methods following the equations developed by Flory and co-workers.[22-24] With the introduction of nonregular sequences of monomers, property averages over both conformation and constitution (constitution referring here to the specific sequence of monomers in the chain which is consistent with the specified average composition) may be approximated by taking the constitution average of the Boltzmann-weighted conformation average of each member of an arbitrarily large sample of chains, each selected at random. We envisage polymerization from a nondepleting monomer pool of fixed composition. Sequences are generated by a first-order Markov process which depends only on the identity of the monomer at the growing end of the chain. In addition, it is taken that reaction proceeds without bias (i.e., there is no tendency toward blockiness due to unequal monomer reactivities) and there is no subsequent rearrangement of monomer (e.g., via a biased transesterification reaction). Under these conditions, only the identity of the active group, acid or alcohol, located at the growing end of the chain influences the identity of the next monomer in the chain; all sequences of a given composition and consistent with continuity of the ester linkages are equally likely.

It has been demonstrated that rotation about the C–O bond of the ester moiety exhibits a minimum in potential energy within ±6° of the trans conformation and a maximum of 5–10 kcal/mol in the cis conformation.[25,26] Limiting our consideration to a single trans state for the ester C–O linkage allows us to treat each monomer as a unit of interdependent potentials with no dependence of conformation extending from one mer to the next. Following Flory,[22] this simplification facilitates the determination of conformation averages which encompass simultaneous statistical weighting both of conformation states and of monomer sequences by matrix multiplication methods.[27]

Each of the monomers considered here consists of a ring group flanked by two terminal groups representing one backbone atom each. However, the conventional replacement of rigid aromatic moieties by a single virtual bond is complicated by the fact that two of the ring groups, the *m*-phenylene and the naphthylene moieties, do not exhibit collinear exocyclic chain continuation bonds. This situation is further complicated by the feature of nonparallel exocyclic bond vectors in the case of the *m*-phenylene moiety; independent rotations about these nonparallel exocyclic continuation vectors require a minimum of two virtual bonds to describe this aromatic moiety. For this reason, and for the sake of internal consistency, all monomers are treated as sequences of four "bonds" each. The first bond includes the preceding ester-ring bond and extends to an arbitrarily selected point along the same line within the ring (e.g., geometric center of the ring in the *p*-phenylene and *m*-phenylene units, and of the first ring in the biphenylene and naphthylene units). The second bond is rigidly constrained to reflect ring planarity and is of zero length in all ring moieties but the 2,6-disubstituted naphthylene unit, where it extends from the center of the first ring to the center of the second ring; this artifice allows us to define the third bond independently of the first, such that it extends from the last position in the ring along a line collinear with the succeeding ring-ester bond. The fourth and final bond is the bridging C–O bond of the ester linkage. Figure 1 illustrates this representation for each of the four ring group types, with the virtual bonds shown as solid lines on the skeleton of the monomer.

We have assumed fixed bond lengths and valence angles in this work. The true interatomic bond lengths and angles employed are listed in Table I; these values were assumed after consideration of data for aromatic polyesters available in the literature.[25,28] Table II shows the bond lengths and bond angles for the multiple virtual bond description of the 16 monomers considered, based on templates of the form X–R–Y and illustrated in Figure 1. These values were derived from those given in Table I. One advantage of the definitions chosen here is the ease of identification of rotations about virtual bonds with the corresponding rotations about real bonds, which simplifies the parameterization of statistical weight matrices.

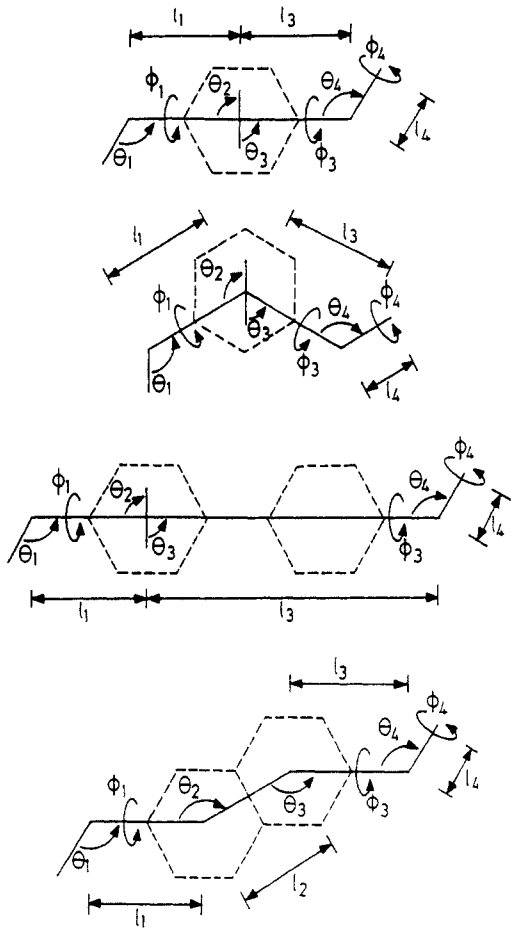

Figure 1. Diagram illustrating the definition of the four virtual bonds comprising each monomer type in the aromatic polyesters with all torsions in the trans conformation. In the first three aromatic moieties the second bond, being of zero length, is not indicated.

Table I
Atomic Bond Lengths and Bond Angles[a]

bond	length (Å)	valence angle	angle (deg)
C*–O	1.37	C_{ar}–C*–O	118.3
C_{ar}–C_{ar}[b]	1.39	C_{ar}–O–C*	110.9
C_{ar}–O	1.41		
C_{ar}–C*	1.49		
C_{ar}–C_{ar}[c]	1.45		

[a] C* refers to the carbonyl carbon, and C_{ar} refers to the ring carbon. [b] 1.39 Å corresponds to the carbon–carbon bond length in the aromatic ring. [c] 1.45 Å corresponds to the carbon–carbon single bond connecting two aromatic rings in the biphenylene moiety.

Assignment of Isomeric States and Statistical Weights. The identification of rotational isomeric states and the corresponding statistical weight matrices was based on the combined consideration of parameters suggested in the literature[25,28] as well as analyses of our own using the semiempirical quantum mechanics software MOPAC[29] with the AM1 Hamiltonians. We performed energy minimizations for models of each of the 16 monomers under consideration; each model compound consisted of a ring group flanked on either side by ester groups of appropriate orientation and capped at either terminus by methyl moieties. In the absence of steric conflicts, the delocalization of π electrons within the ester group and each of the ring groups causes these moieties to favor planar conformations both individually and in pairs. Symmetry considerations lead us to anticipate up to four local minima in energy for torsion about any bond connecting two such planar species. Energetic coupling between groups separated by two or more bonds (e.g., the ester groups attached to the exocyclic bonds of a ring group) can lead to shifts in the location or relative energy of these minima.

Table II
Lengths of and Valence Angles between Virtual Bonds for Polyacrylate Monomers As Illustrated in Figure 1 and Described by the Template X–R–Y[a]

		bond length, Å			
bond		R = *p*-phenylene	R = *m*-phenylene	R = biphenylene	R = naphthylene
X = C(O)	l_1	2.88	2.88	7.11	4.27
X = O	l_1	2.80	2.80	7.03	4.19
R	l_2	0.0	0.0	0.0	1.39
Y = C(O)	l_3	2.88	2.88	7.11	4.27
Y = O	l_3	2.80	2.80	7.03	4.19
X–Y	l_4	1.37	1.37	1.37	1.37
		angle, deg			
angle[b]		R = *p*-phenylene	R = *m*-phenylene	R = biphenylene	R = naphthylene
X = C(O)	θ_1	118.3	118.3	118.3	118.3
X = O	θ_1	110.9	110.9	110.9	110.9
R	θ_2	90	120	90	150
R	θ_3	90	60	90	150
Y = C(O)	θ_4	118.3	118.3	118.3	118.3
Y = O	θ_4	110.9	110.9	110.9	110.9

[a] X and Y are elements of the ester group, R designates the identity of the aromatic ring group, and X–Y is the C(O)–O bond of the ester linkage connecting successive monomers. Lengths of virtual bonds are derived by simple geometry from the basic atomic bond lengths provided in Table I. [b] The numbering of bond angles differs slightly from that employed elsewhere (ref 22). Refer to figure 1 for clarification.

In all cases where the carbonyl carbon was bonded directly to the ring, two equal energy local minima were observed, wherein the carbonyl bond lies coplanar with the ring plane. Where two such carbonyls were bonded to the same ring group, we found no evidence of coupling between these two rotations. In cases where one carbonyl carbon and one ester oxygen were bonded directly to the ring, the carbonyl remained coplanar with the ring and four equal energy local minima were observed for rotation about the ring–oxygen bond, corresponding to out-of-plane rotations of 45–50°; again, there was no indication of coupling across the ring with the opposing carbonyl–ring rotation. Lastly, model compounds containing two ester oxygens bonded directly to the ring exhibit 16 isomeric states, each ring–oxygen bond rotation assuming one of four minimum energy positions. The AM1 calculations suggested a weak coupling (~1 kcal/mol) between these opposing ring–oxygen rotations in monomers containing *p*-phenylene and naphthylene which favors anti orientation of the ester linkages across the plane of the ring. In *m*-phenylene, this coupling is especially strong, to the extent that the out-of-plane rotation of the ester groups shifts in some cases to 50° or 55° and exhibits conformation energies 1.5 kcal/mol in excess of the minimum energy conformation.

Further investigation using the ab initio package GAUSSIAN 86 with the STO-3G basis set[30] of the energies of the model compounds involving *p*-phenylene bonded to two ester oxygens confirmed the 4-fold conformational stability of the ring-ester dihedral but failed to substantiate either the energetic coupling or the alteration of bond dihedrals suggested by the AM1 calculations. Given this discrepancy, we were unable to resolve unambiguously the true extent of across-ring interactions in this instance. The calculations of Lautenschläger et al.[26] suggest a further discrepancy between AM1 and STO-3G results for the relative energies of cis and trans conformations for two carbonyls bonded to a common ring. One solution may

Table III
Isomeric State Assignments and Statistical Weight Matrices for Rotational Isomers about Virtual Bonds for Polyarylate Monomers As Illustrated in Figure 1 and Described by the Template X-R-Y[a]

Conventional RIS Model

	bond 4'[b] Y = O	bond 1 Y = O	bond 3 Y = C(O)	bond 3[c] Y = O
X = C(O)				
ϕ_i (deg)	0	0, 180	0, 180	45, 135, −135, −45
U_i[d]	$\begin{bmatrix}1\\1\\1\\1\end{bmatrix}$	$\begin{bmatrix}1 & 1\end{bmatrix}$	$\begin{bmatrix}1 & 1\\1 & 1\end{bmatrix}$	$\begin{bmatrix}1 & 1 & 1 & 1\\1 & 1 & 1 & 1\end{bmatrix}$
X = O				
ϕ_i (deg)	0	45, 135, −135, −45	0, 180	45, 135, −135, −45
U_i[d]	$\begin{bmatrix}1\\1\end{bmatrix}$	$\begin{bmatrix}1 & 1 & 1 & 1\end{bmatrix}$	$\begin{bmatrix}1 & 1\\1 & 1\\1 & 1\\1 & 1\end{bmatrix}$	$\begin{bmatrix}\alpha & \beta & \gamma & \alpha\\ \gamma & \alpha & \alpha & \gamma\\ \gamma & \alpha & \alpha & \gamma\\ \alpha & \gamma & \beta & \alpha\end{bmatrix}$

Variance RIS Model

	bond 4'[b,e] Y = O	bond 1 Y = O	bond 3 Y = C(O)	bond 3[c] Y = O
X = C(O)				
ϕ_i (deg)	0, +δ, −δ	0, 180	0, 180	45, 135, −135, −45
U_i[d]	$\begin{bmatrix}1 & \zeta & \zeta\\1 & \zeta & \zeta\\1 & \zeta & \zeta\\1 & \zeta & \zeta\end{bmatrix}$	$\begin{bmatrix}1 & 1\\1 & 1\\1 & 1\end{bmatrix}$	$\begin{bmatrix}1 & 1\\1 & 1\end{bmatrix}$	$\begin{bmatrix}1 & 1 & 1 & 1\\1 & 1 & 1 & 1\end{bmatrix}$
X = O				
ϕ_i (deg)	0, +δ, −δ	45, 135, −135, −45	0, 180	45, 135, −135, −45
U_i[d]	$\begin{bmatrix}1 & \zeta & \zeta\\1 & \zeta & \zeta\end{bmatrix}$	$\begin{bmatrix}1 & 1 & 1 & 1\\1 & 1 & 1 & 1\\1 & 1 & 1 & 1\end{bmatrix}$	$\begin{bmatrix}1 & 1\\1 & 1\\1 & 1\\1 & 1\end{bmatrix}$	$\begin{bmatrix}\alpha & \beta & \gamma & \alpha\\ \gamma & \alpha & \alpha & \gamma\\ \gamma & \alpha & \alpha & \gamma\\ \alpha & \gamma & \beta & \alpha\end{bmatrix}$

[a] X and Y are elements of the ester group, R designates the presence of the aromatic ring group, and X–Y is the C(O)–O bond of the ester linkage between successive monomers. The present RIS parameterization is not sensitive to the identity of the aromatic group, each of which is assumed to be rigid and planar. [b] Bond 4' corresponds to the ester linkage bond of the preceding monomer; the form of U_4 for each monomer depends on the identity of X in its successor, so $U_{4'}$, is presented here. [c] There is some evidence for coupling across the ring in hydroquinone and resorcinol monomers; where this coupling is specifically referred to in the text, α, β, and γ take on the following values, respectively: 1.0, exp(−500/T), exp(−500T) in hydroquinone and exp(−500/T), exp(−750/T), 1.0 in resorcinol. Otherwise, $\alpha = \beta = \gamma = 1$. [d] U_2 is the identity matrix $\mathbf{E}_s$ of order s, where s is the number of columns in U_1 or the number of rows in U_3. [e] $\delta = 53°$ and $\zeta = \exp(-900/T)$. Refer to text for details.

be to resort to successively higher level basis sets in the ab initio calculations. However, in the absence of corroborating experimental evidence, it is difficult to verify any improvements in accuracy in return for the significantly greater computational complexity. Compounds with large dipoles and significant electron delocalization appear to be especially problematic. That higher level basis sets may actually overestimate such interactions in aromatic species has been documented in the literature.[31] The detailed evaluation of computational methods for estimating molecular properties, however, constitutes a topic in its own right and is beyond the scope of the present analysis. At this stage, we have opted for a representation involving four isomeric states for each ring–oxygen bond, with statistical weights assigned which ignore possible coupling between ring-oxygen rotations consistent with the results from calculations at the STO-3G basis set level. Later on we consider the ramifications of this assignment in greater detail by means of a sensitivity analysis which takes into consideration the discrepancies between computational methods and the ambiguity in isomeric state location.

For the conformation of the ester group, we consider the model compound *p*-phenoxybenzoate; our results are similar to those reported by Coulter and Windle,[25] confirming an energy minimum for the trans ester conformation. A second minimum was determined for the ester C–O bond with a twist of 25° out of the cis-planar conformation, with significant cooperative twists at the ester–phenylene bonds. However, the energies of these latter conformations are more than 5 kcal/mol higher than the most stable trans conformation, and their likelihood may be further reduced by long-range intramolecular steric exclusion. For this reason we deem it reasonable to assume, without loss of accuracy, a single isomeric state for this ester bond, as has been previously done in studies of poly(ethylene terephthalate),[32] which justifies analysis based on the assumption of independently configurable monomers.

The final selection of isomeric states and the corresponding statistical weight matrices are presented in Table III. Statistical weights are based on minimum energy conformations alone, neglecting possible differences in curvature of the energy surface in the vicinity of the minima. This approximation is believed to be justified on the basis of the symmetry of the molecules involved and the already inherent degree of approximation incurred in our representation of the ring–oxygen bond. Where employed in calculations, coupling between ring–oxygen bonds, which affects only those compositions containing diol monomers, is effected by altering the statistical weights assigned to U_3, as illustrated in Table III; U_2 is the identity matrix. These are described more fully in the footnotes to Table III.

Scaling Length. In order to make comparisons between results calculated for the various compositions within the polyester family, it is essential to scale the calculations in an appropriate and self-consistent manner. For a chain molecule such as a polyalkane consisting of an uninterrupted sequence of like bonds, it is straightforward to recognize an appropriate scaling length in the 1.54 Å of the C–C bond. For regular chains which consist of repeating sequences of bonds, such as Nylon 6 or the polyester PPT, one can deduce rigorously the appropriate scaling length from the nonreducible constitutional subunit, as demonstrated by Erman et al.[33] For a regular copolymer whose repeat unit consists of a fixed sequence of N bonds, one has

$$\ell^* = \frac{1}{N}[\mathbf{l}_1 + \langle \mathbf{T}_1 \rangle \mathbf{l}_2 + \ldots + \langle \mathbf{T}_1 \mathbf{T}_2 \ldots \mathbf{T}_{N-1} \rangle \mathbf{l}_N] \quad (1)$$

where ℓ^* is the scaling vector, the magnitude l of which is the scaling length; the definition employed by Erman et al. is a special case of eq 1; $\mathbf{l}_i$ and $\mathbf{T}_i$ are the bond vector and internal transformation matrix defined elsewhere.[22] For nonregular chain constitutions, however, one requires a more general definition of scaling length. By analogy to eq 1, we propose a similar scaling relation where ℓ^* is averaged over all possible sequences of N bonds, N being the product of the number of monomer types m and the number of bonds per monomer. For chains with independent rotation potentials between monomers, this simplifies to a summation involving vectors spanning individual monomers and transformation matrices for each

monomer type in place of individual bond vectors and bond axis transformation matrices:

$$l^* = \frac{1}{m}\sum_{a=1}^{m}\sum_{b=1}^{m}\cdots\sum_{z=1}^{m} c_a w_{a,b} w_{b,c}\cdots w_{m-1,m}[\mathbf{l}_a + \langle \mathbf{T}_a\rangle \mathbf{l}_b + \ldots + \langle \mathbf{T}_a\mathbf{T}_b\ldots\mathbf{T}_{m-1}\rangle \mathbf{l}_m] \quad (2)$$

c_a is the concentration of the ath group of bonds (i.e., monomer a), and w_{ab} is the transition probability from monomer a to monomer b. The number (z) of summations and the number (m) of terms in each summation are equal to the number of monomer types (typically two or three) comprising the random copolymer. The scaling vector so defined reflects the probability of observing each m-mer sequence in the copolymer of degree of polymerization $n \geq m$ and weights the corresponding contribution to the scaling length accordingly. It may be readily shown that eq 1 is a special case of eq 2, wherein w_{ij} takes only values of zero or unity and one assumes the identity of the initial monomer in the chain ($c_1 = 1$). The scaling length l^* thus defined is characteristic of the composition and is independent of chain length.

Measures of Chain Conformation. The conventional rotational isomeric state (RIS) implementation thus far described has been applied to several representative members of the polyester family covering a broad range of observed behavior. For each composition, the results may be summarized by the scaling length l^*, the scaled magnitude of the mean persistence vector $|\langle \mathbf{r}\rangle|/l^*$, and the scaled mean square end-to-end distance $\langle r^2\rangle/nl^{*2}$, or characteristic ratio C_n. Both of these averages necessarily converge asymptotically to limiting values at high degrees of polymerization. Brackets are used here to indicate averages taken simultaneously over all allowed conformations as well as all constitutions (i.e., monomer sequences) of the chain. The average radius of gyration tensor $\langle \mathbf{S}_{x2}\rangle$ determined in the frame of reference of the first two bonds of the chain is computed and transformed to the principle axis system by diagonalization such that

$$\langle \mathbf{S}_{x2}\rangle = \mathrm{diag}(\lambda_1,\lambda_2,\lambda_3) \qquad \lambda_3 \geq \lambda_1 \geq \lambda_2 \quad (3)$$

From this an additional measure of chain size is obtained in the form of the mean squared radius of gyration, the first invariant of the $\langle \mathbf{S}_{x2}\rangle$ tensor.

$$\langle s^2\rangle = \mathrm{tr}(\langle \mathbf{S}_{x2}\rangle) = \lambda_1 + \lambda_2 + \lambda_3 \quad (4)$$

For the evaluation of shape anisotropy, we follow the analysis of Theodorou and Suter[34] in defining analogous parameters for the asphericity b, acylindricity c, and relative shape anisotropy κ^2 of the average radius of gyration tensor:

$$b = \lambda_3 - \frac{1}{2}(\lambda_1 + \lambda_2) \qquad b \geq 0$$

$$c = \lambda_1 - \lambda_2 \qquad c \geq 0 \quad (5)$$

$$\kappa^2 = \frac{(b^2 + (3/4)c^2)}{(\langle s^2\rangle)^2} \qquad 0 \leq \kappa^2 \leq 1$$

These parameters derive from the traceless deviatoric part of $\langle \mathbf{S}_{x2}\rangle$:

$$\hat{\mathbf{S}} = \langle \mathbf{S}_{x2}\rangle - \frac{1}{3}\mathrm{tr}(\langle \mathbf{S}_{x2}\rangle)\mathbf{E}_3 = b\,\mathrm{diag}\left(\frac{-1}{3},\frac{-1}{3},\frac{2}{3}\right) + c\,\mathrm{diag}\left(\frac{1}{2},\frac{-1}{2},0\right) \quad (6)$$

$\mathbf{E}_3$ is the unit tensor of rank three. For shapes of tetrahedral or higher symmetry, both b and c are zero; for shapes of cylindrical symmetry, only c equals zero. The relative shape anisotropy κ^2 varies from an upper limit of unity, for rodlike molecules, to one-quarter for uniform planar arrays of atoms, to a lower limit of zero for structures of tetrahedral or higher symmetry. At sufficiently high degrees of polymerization, each polyester type approaches Gaussian coil behavior, characterized by a Kuhn segment length l_K. This approach to Gaussian coil behavior may be marked by isotropization of $\langle \mathbf{S}_{x2}\rangle$: The three diagonal elements λ_1, λ_2, and λ_3 become equal and the asphericity, acylindricity, and relative shape anisotropy all decrease to zero. Our interest lies in their variation with segment length for subunits of the polymer chain.

A second set of measures originally employed by Šolc[35] is specified by the eigenvalue ratios λ_1/λ_3 and λ_2/λ_1, the first of which is unity for oblate ellipsoids and the latter of which is unity for prolate ellipsoids; spheres are characterized by both ratios being unity, while rods are characterized by λ_1/λ_3 equal to zero and λ_2/λ_1 equal to unity.

Table IV
Scaling Lengths (Å) Determined for Polyesters of Various Composition

polymer	l^*	polymer	l^*	polymer[a]	l^*
PHNA	8.309	HIQ-99	6.141	HBA/TA/ND	6.928
BN-33	7.546	HIQ-98	6.111	HBA/TA/BP/HNA	6.581
BN-50	7.197	HIQ-95	6.022	HBA/TA/RL 25	4.723
BN-67	6.848	HIQ-74	5.408	TA/RL	4.759
PHBA	6.245	HIQ-60	5.012	mHBA/TA/HQ 25	4.828
PPT	6.245	HIQ-50	4.741	mHBA/TA/HQ 50	3.758
		HIQ-34	4.328	HBA/mHBA 25	4.827
		HIQ-20	3.993	HBA/mHBA 50	3.758
		PPI	4.792		

[a] These are special compositions; refer to text for details

Results

Rodlike Polyesters. The first of the compositions under consideration include the regular p-phenylene-based homopolyesters of HBA and of terephthalic acid (TA) and HQ (denoted PPT), investigated originally by Erman et al.[33] and designated type I and type II polyesters, respectively; coincidental with these within a precision of 1% are the results of calculations for nonregular compositions consisting of various combinations of HBA, comprising x% of the polymer, and TA and HQ, each comprising $(100 - x)/2$% of the polymer. Our results for persistence vector and mean square end-to-end distance by conventional RIS methods accord quantitatively with values reported previously. In all respects, the behavior of the PPT chains and all intermediate nonregular compositions of HBA/TA/HQ mimic that of PHBA chains; it suffices to report only results for PHBA.[36] The scaling lengths determined by eq 2 for this and several other polymer compositions are indicated in Table IV. The limiting scaled values for the magnitude of the mean persistence vector, the characteristic ratio, and the radius of gyration for PHBA are listed in Table V. Also reported in Table V are the calculated persistence lengths a for the Porod–Kratky model, determined using

$$a = (l^*/2)(C_\infty + 1) \quad (7)$$

For a polymer of sufficient length to approximate a random coil, by the Kuhn hypothesis, the ratio of $\langle r^2\rangle/\langle s^2\rangle$ should approach a value of 6; a value of 7.34 is attained for PHBA by a degree of polymerization of 1025, and 6.17 is attained by a degree of polymerization of 8193. This slow convergence and the high limiting values listed in Table V for

Table V
Limiting Values[a] of the Scaled First and Second Moments (i.e., Characteristic Ratio) of the End-to-End Vector and Radius of Gyration for PHBA and the HIQ Compositions, and Corresponding Persistence Lengths

composition	$[\|\langle \mathbf{r} \rangle\|/l^*]_\infty$	C_∞	a (Å)	$[\langle s^2 \rangle/nl^{*2}]_\infty$
PHBA[b]	120	236	740	38.3
HIQ-99	92.0	185	571	30.2
HIQ-98	73.6	149	458	24.4
HIQ-95	46.2	95.2	290	15.7
HIQ-74	13.7	31.4	87.6	5.23
HIQ-60	9.74	24.2	63.2	4.02
HIQ-50	8.24	21.6	53.6	3.60
HIQ-34	6.78	19.4	44.1	3.24
HIQ-20	5.99	18.6	39.1	3.09
PPI	3.91	10.1	26.6	1.68

[a] Based on calculations for a degree of polymerization of 8193. [b] All BN compositions are similar (with the exception of values for persistence length a).

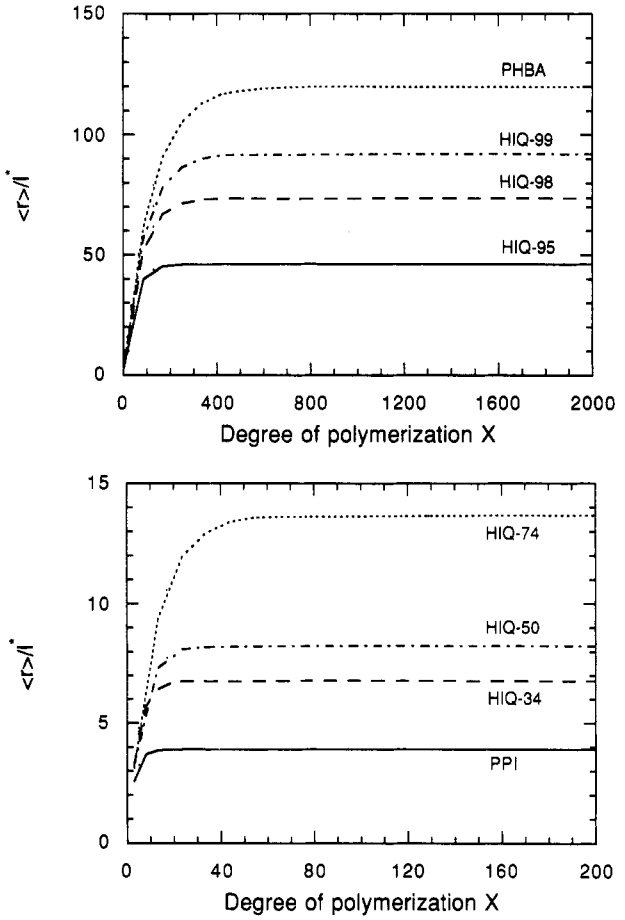

Figure 2. Mean magnitude of the persistence vector $\langle \mathbf{r} \rangle$ scaled by the corresponding scaling length l^* taken from Table IV for PHBA and several HIQ compositions. The curve for PHBA is representative of all the stiff-chain polymers, including those composed of HBA and HNA: (a, top) rodlike compositions containing less than 10% angular disruptor units; (b, bottom) coiling polymers containing greater than 10% angular disruptor units. Note the differences in axis scaling.

PHBA testify to its extreme rigidity. As noted previously by Erman et al., because of the collinearity of the chain propagation bonds at the rings in PPT and PHBA the ultimate persistence length and characteristic ratios are determined largely by the 7.4° difference between the two bond angles of the ester group and are quite sensitive to small changes in this difference. The chain length dependences of $|\langle \mathbf{r} \rangle|/l^*$ and C_n for PHBA are included in Figure 2 and Figure 3, respectively. The asphericity and relative shape anisotropy, normalized by $\langle s^2 \rangle$, are plotted

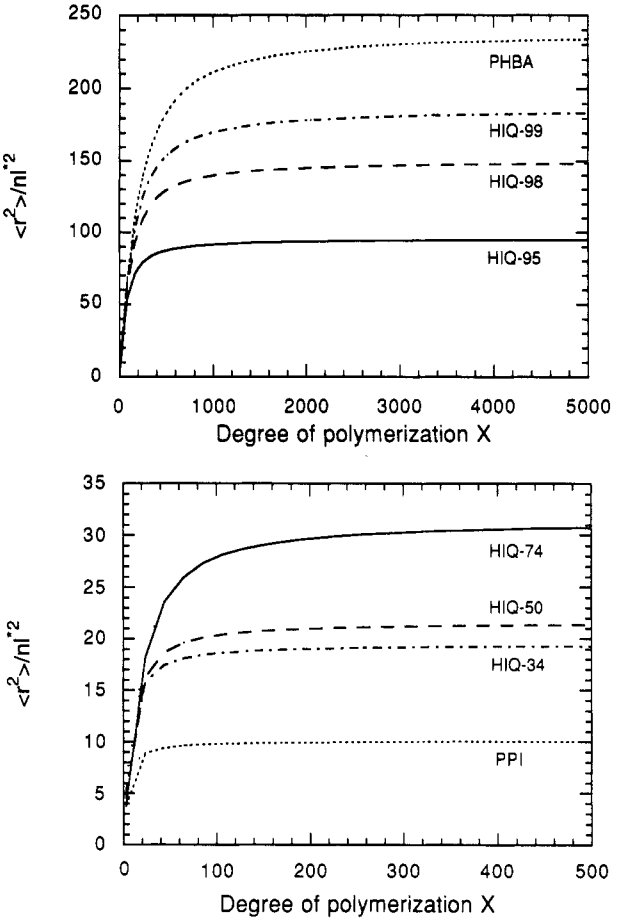

Figure 3. Characteristic ratio C_n for PHBA and several HIQ compositions. The curve for PHBA is representative of all the stiff-chain polymers, including those composed of HBA and HNA: (a, top) rodlike compositions containing less than 10% angular disruptor units; (b, bottom) coiling polymers containing greater than 10% angular disruptor units. Note the differences in axis scaling.

as functions of inverse chain length in Figure 4. The Šolc ratios λ_1/λ_3 and λ_2/λ_1 provide another measure of chain shape and its change with increasing degree of polymerization (Figure 5). From Figure 4 and Figure 5, the asphericity and prolate ellipsoidal character of PHBA and PPT suggest that these materials retain a major portion of their rodlike character in segments up to 20 mers long, due entirely to short-range intramolecular forces.

In the second instance, we consider the family of BN copolymers, each member being designated by its percentage content of HBA monomer. These are obviously closely related to the PHBA homopolymer already considered, which represents the BN-100 composition. Calculations for compositions of BN-67, BN-50, BN-33, and BN-0 (PHNA) suggests that these materials are all very similar in their single-chain characteristics. Differences may be summarized entirely by the variation in scaling length, which increases with increasing HNA content as indicated in Table IV. The single-chain behaviors, after appropriate scaling, described as functions of the degree of polymerization as in Figures 2–4, all fall along curves almost identical to that for PHBA, deviations in all respects being less than 3%. The increase in scaling length with increasing HNA content is an obvious result of the increasing contribution from the longer HNA monomer and suggests longer persistence lengths and actual chain dimensions, but shape anisotropies for these materials essentially identical to those for PHBA.

Two special cases of the class of rodlike polyesters which were considered are the terpolymer of HBA, TA, and 2,6-

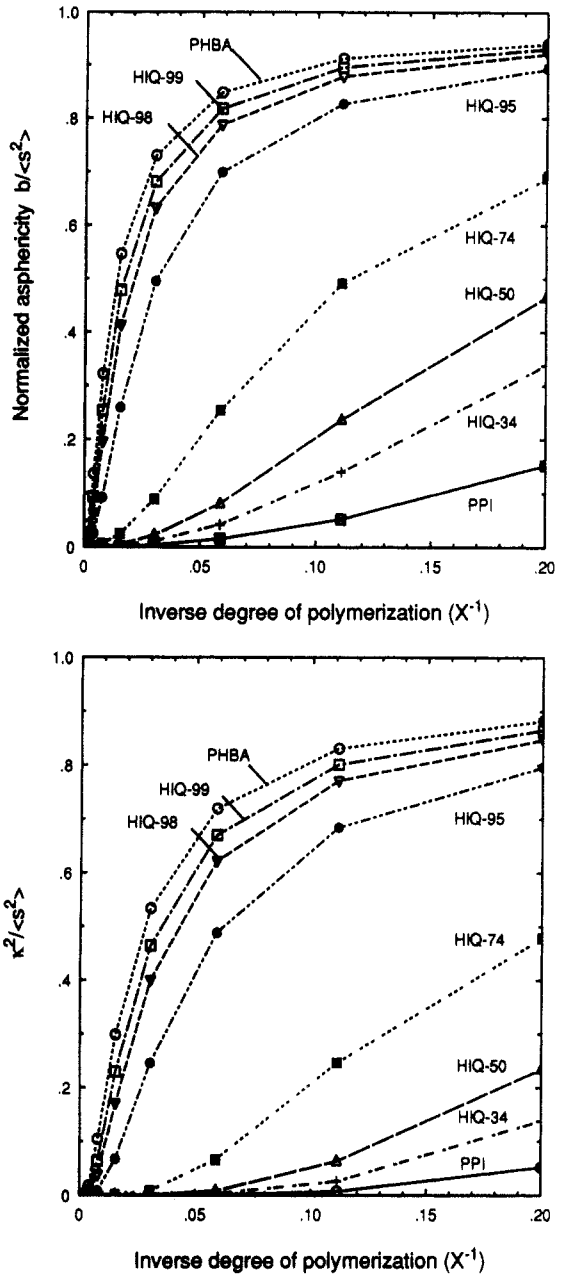

Figure 4. Shape factors derived from the average radius of gyration tensor, normalized by the first invariant of the tensor, plotted against inverse degree of polymerization, to illustrate deviation from rodlike behavior: (a, top) normalized asphericity vs X^{-1}; (b, bottom) relative shape anisotropy vs X^{-1}.

naphthylenediol (ND), combined in proportions 3:1:1 and a four-component material composed of HBA, TA, 4,4′-biphendiol (BP), and HNA, in proportions 12:3.5:3.5:1. These materials have been investigated in dynamic mechanical tests reported elsewhere.[11] The first of these was originally proposed in an attempt to improve the copolyester processability through further disruption of chain order and the breakdown of intermolecular sequence correlations as the result of introducing symmetric difunctional monomers; one would expect this to introduce little or no change from the conformational behavior observed for the BN copolymers. The second polymer composition was proposed in an attempt to improve the longitudinal mechanical properties of the final fiber product through the introduction of what was considered to be a more effective mesogenic unit, the biphenylene moiety. The scaled behavior of these two materials fall within 5% of that observed for PHBA. The scaling lengths, reported in Table IV, for these particular compositions

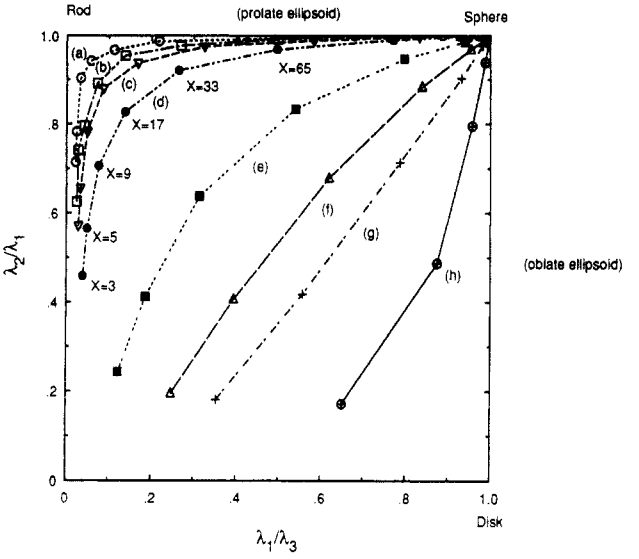

Figure 5. Chain shape described by the average radius of gyration tensor, expressed as a plot of the ratios of its eigenvalues: (a) PHBA, (b) HIQ-99, (c) HIQ-98, (d) HIQ-95, (e) HIQ-74, (f) HIQ-50, (g) HIQ-34, (h) PPI.

vary within the range previously encompassed by the BN compositions. It may be concluded that, given these scaling lengths and the similar behavior of these and the BN family of polymers, one would expect the isolated chains of these polymers to mimic (roughly) BN-80 and BN-65.

Polyesters with Angular Disruptor Units. Somewhat different behavior from that of the so-called rodlike polyesters is exhibited by the group of polyesters containing angular disruptor units. These generally consist of monomers identical to those used to synthesize rodlike chains, with the added contribution of some fraction of monomers containing the *m*-phenylene moiety, a unit which introduces a local 60° deflection in the chain contour direction wherever it occurs in the polymer backbone. Introduced in a nonregular manner into the chain backbone and left uncompensated, these angular disruptions promote a higher degree of curvature along the chain contour and further frustrate efficient intermolecular packing of chains in the bulk. Most important of this class of materials are the HIQ compositions, which have already been the object of much investigation.

The scaling lengths for several HIQ compositions ranging from 50% *m*-phenylene content to only 0.5% *m*-phenylene content are reported in Table IV; the nomenclature indicates the *x*% HBA content, with the remainder being evenly split between $(100 - x)/2$% each of IA and HQ. Within this group, scaling length decreases with increasing content of angular disruptor units until one reaches the limiting case of the alternating copolymer PPI, where a very slight upturn is observed.

The chain length dependences for $|\langle \mathbf{r} \rangle|/l^*$ and C_n for the HIQ materials are illustrated in Figure 2 and Figure 3, with values for $[|\langle \mathbf{r} \rangle|/l^*]_\infty$ and C_∞ provided in Table V. The most obvious observation is the striking drop in apparent chain rigidity, as measured by characteristic ratios and persistence lengths, resulting from the introduction of only 5–10% angular disruptor units in the polymer composition; by ~7.5% IA content, the persistence length has dropped to less than 10% of its pure PHBA value. Because it is the allowed rotation about the noncollinear bonds of the *m*-phenylene moiety which dominates this behavior, the results reported for the HIQ compositions are not as sensitive to small variations in the assignment of bond angles in the ester group as was noted

Table VI
Limiting Values for Compositions of Polymers Containing Different Angular Disruptor Units[a]

polymer	$[\lvert\langle \mathbf{r}\rangle\rvert/l^*]_\infty$	C_∞	a (Å)	$[\langle s^2\rangle/nl^{*2}]_\infty$
TA/RL	3.91	10.1	26.4	1.69
HBA/TA/RL 25	8.23	21.6	53.4	3.60
mHBA/TA/HQ 50	5.75	18.9	37.4	3.15
mHBA/TA/HQ 25	9.22	23.7	59.6	3.95
HBA/mHBA 50	5.75	18.9	37.4	3.15
HBA/mHBA 25	9.22	23.7	59.6	3.95

[a] The polymers listed in this table are special compositions; refer to text for details.

for the more rigid materials. The rapid conversion to coiled polymer behavior may be observed in each of the calculated parameters and is illustrative of the obvious distinction between single-chain behavior in the kinked-chain HIQ and the rodlike aromatic polyesters previously discussed.

The shape factors for the various HIQ compositions are demonstrated in Figures 4 and 5, alongside those for PHBA. In these cases, the polymer chain exhibits a monotonic decline in inherent rigidity, even over very short segment lengths in materials with appreciable *m*-phenylene content. Again, this transition is most striking between 0% and 7.5% IA. Only below roughly 10% *m*-phenylene units does the chain obtain even 80% aspheric character, with the transition to rigid segment behavior occuring rapidly as one eliminates the *m*-phenylene content. For the large range of HIQ compositions, including all those of technical interest to date, the inherent short-range chain behavior is far from rodlike. For these materials to be simulated in the solid state as rodlike structures, one must assume considerable ordering influence from intermolecular interactions or externally imposed forces.

For comparison with the HIQ single-chain results, variations in the detailed nature of the angular disruptor unit were also considered. These entailed compositions wherein the angular disruptor unit consisted of *m*-hydroxybenzoate (mHBA) or 1,3-dihydroxybenzene (resorcinol, RL). For brevity, we limit discussion to a few illustrative compositions containing either 50% angular disruptor units (analogous to PPI) or 25% angular disruptor units (analogous to HIQ-50). Thus we consider materials composed of the following monomer combinations: HBA/TA/RL, mHBA/TA/HQ, and HBA/mHBA; composition nomenclature deviates from the convention previously introduced for HIQ in that the numeric values refer to the percentage content of the *m*-phenylene monomer, thus emphasizing the content of disruptor units involved.

For each of these six polymers, the calculated scaling lengths and asymptotic scaled behaviors are listed in Tables IV and VI, respectively. It has been suggested[18] that the uncorrelated twist about the ring–oxygen bonds of the resorcinol monomer in HBA/TA/RL distinguishes this polymer from that containing terephthalic acid, a planar moiety, in combination with hydroquinone. However, our results suggest that, under the sole influence of short-range intramolecular interactions, the single-chain behavior of HBA/TA/RL is essentially identical to that observed for HIQ in the range from 0% to 50% HBA content; what differences exist are reflected largely in the 2% discrepancy in scaling lengths and are not reflected in considerations of rigidity or chain anisotropy. We conclude that any observed differences between the HBA/TA/RL family of polymers and the HIQ materials must arise, at least indirectly, as a result of chain-packing considerations or external forces. In contrast to this close similarity between HIQ and HBA/TA/RL, the polymers containing *m*-hydroxybenzoic acid, mHBA/TA/HQ and HBA/mHBA, appear to be marginally stiffer than HIQ and HBA/TA/RL, as evidenced by slightly higher persistence lengths. However, this difference is relatively small compared to that induced by eliminating the kinked units altogether. One might expect such differences to be insignificant when considered in the presence of intermolecular interactions.

Sensitivity Analysis. Because of the discrepancy between the predictions of conformational energies of the diol monomers using MOPAC and those suggested by calculations using GAUSSIAN 86, it is important to assess the significance of small deviations in statistical weight assignments to the reported results, especially in the case of PPT and the HIQ materials, which contain the diol monomer. The calculations were repeated using the U_3 matrices listed in Table III for hydroquinone with α, β, and $\gamma \neq 1$; these values were deduced from the coupling suggested by AM1 calculations and are listed at the bottom of Table III. In the case of the relatively stiff chain PPT, one observes a strong dependence of asymptotic limiting values on the elements of U_3; the assignment of a 1 kcal/mol difference between syn and anti arrangements of the two ester groups about the intervening ring results in a decrease in l^* from 6.245 to 6.220 Å but reductions in both $[\lvert\langle \mathbf{r}\rangle\rvert/l^*]_\infty$ and C_∞ by 25%. PPI and HIQ materials, on the other hand, are relatively insensitive to this variation of statistical weights; introduction of coupling produces less than a 2% drop in scaling length l^* and C_∞ at 50% HBA content.

The sensitivity of the calculations to the assignment of the ring rotation angle about the ring–oxygen bond was explored by repeating the calculations using isomeric states wherein the ester group is rotated 60° out of the ring plane when connected to the ring by the ester oxygen. These calculations indicate that the results are relatively insensitive to discrepancies of ±15° in the assignment of rotation angle. These results all fell within 1% of those previously discussed for degrees of polymerization greater than 10. However, this insensitivity may well be attributed to specific features of the chains considered here, namely, to the collinear or near-collinear nature of the exocyclic continuation vectors in the rodlike chains, and to the rapid isotropization of conformational properties at low degrees of polymerization in the chains with angular disruptor units.

Comparison to Experimental Data. The high-temperature melt transitions and poor solubility of many of the polyarylates make acquiring reliable experimental data on chain conformation a difficult task. Tsvetkov and coworkers[37,38] have reported values for the Kuhn statistical segment length for some para-linked and meta-linked aromatic polyesters in dilute solution. They synthesized model compounds and polymers of TA and phenylhydroquinone (I) and of the regular repeating sequence $-[-(HBA)_3-mHBA-]_x-$ (II). These materials, in solution with dichloroacetic acid, were studied by diffusion, flow viscometry, and flow birefringence, from which they deduced the Kuhn statistical segment lengths for polymers I and II of 380 ± 50 and 120 ± 20 Å, respectively. These correspond roughly to persistence lengths of 190 Å for I and 60 Å for II. Krigbaum and Tanaka[39] have also reported studies of I by static light scattering, with persistence lengths determined to be ~100 ± 30 Å. By comparison, the RIS method predicts values of 740 Å for PHBA and PPT, or almost 4 times the higher experimental value for I. Krömer et al.[40] reported similar measurements for another stiff-chain composition, BN-70, from which they

deduced a persistence length of 120 ± 10 Å, which again is considerably less than the rigid-rod RIS value of 810 Å.

For comparison to II we draw upon our RIS calculations for a kinked-chain polymer having 25% *m*-phenylene content, such as HIQ-50. In this case, the calculated values correspond to a polymer whose *average* distance between kinked units is four rings, whereas the experimental polymer II is a regular polymer with a kinked unit every fourth ring. Nevertheless, the predicted persistence length of 53.6 Å for HIQ-50 is in reasonable agreement with the data of Tsvetkov et al. for II within the limits of experimental certainty for that polymer. Other investigators[41,42] have determined persistence lengths for HIQ-36 in dilute solution with trifluoroacetic acid/dichloromethane cosolvent by light scattering and in the quenched melt by small-angle neutron scattering. Their results suggest persistence lengths for this material ranging around 10 Å, increasing to as high as 55 Å in the solid state after low-temperature annealing; by comparison, our calculations for HIQ-34 suggest a persistence length of 44.1 Å.

Higher Moments of the Torsion Angle Distribution

Discrepancies between experimental values of persistence length and those calculated by RIS suggest that the present treatment tends to overestimate the chain rigidity, this effect being more pronounced for the rodlike polyester compositions. This overestimation is largely due to two effects, one associated with the selection of fixed bond angles in the ester linkage and the second associated with the assumption of a single rigid trans isomeric state for the ester linkage. Molecular dynamics simulations of short chains of PHBA[43] have emphasized the importance of dynamic fluctuations in bond dihedrals in some stiff-chain polyesters. To account for this we modify the RIS treatment to include additional thermally activated isomeric states in the vicinity of the local minima. This modification is consistent with the treatment of the isomeric state method as a discretization of the continuous distribution of rotation states on the potential energy surface accessible to a given bond torsion. An example of such a potential energy surface based on extensive semiempirical quantum mechanics calculations for model compounds of PHBA has been recently reported by Lautenschläger et al.[26] These results as well as those of Coulter and Windle[25] suggest that whereas the trans conformation is the only important local minimum for the ester torsion, there is some freedom for fluctuation of this angle about its mean value. Furthermore, the evidence indicates that this fluctuation within ±90° of the trans state is roughly independent of torsions about neighboring ester–ring bonds, all ester torsions outside of this range being in excess of 5 kcal/mol higher in energy than the minimum energy state. Thus it is perfectly adequate to assign isomeric states for the ester torsion ϕ_{ester} and the corresponding statistical weights based solely upon the potential energy dependence of this torsion alone. This energy, in turn, is reasonably well approximated by an analytical function of the form

$$E_{ester} = \frac{\kappa}{2}(1 + \cos(2\phi_{ester} - \phi_0)) \qquad |\phi_{ester}| \le 90° \tag{8}$$

$$E_{ester} = \kappa \qquad 90° \le |\phi_{ester}| \le 180°$$

where κ is ~5 kcal/mol and ϕ_0 is 180°.

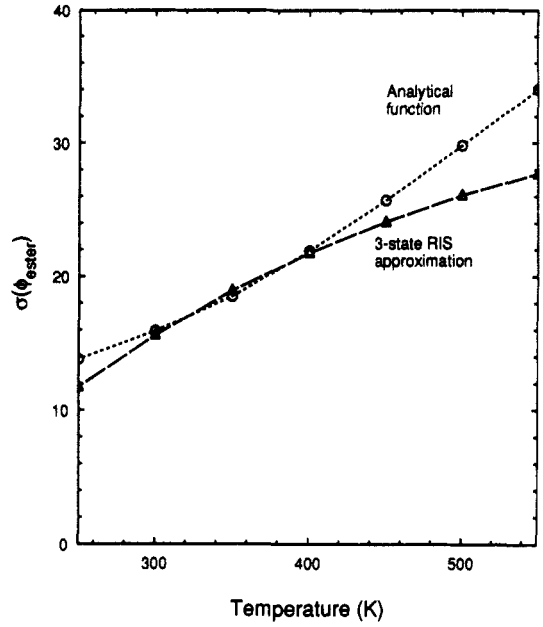

Figure 6. Standard deviation (in degrees) of the distribution of the ester torsion ϕ_{ester} about the energy minimum at $\phi_{ester} = 0°$ over the temperature range of interest: (○) eq 8; (△) three-state RIS approximation.

In common practice, isomeric states are assigned in accordance with the number of local minima observed in the potential energy profile or surface; alternatively, isomeric states are assigned at uniform intervals in torsion angle, their number being determined by the angular resolution desired. In this approach, we seek to reproduce the character of the torsion angle distribution up to its second moment with a minimal cost in computational complexity. To do this, we discretize this function to reproduce the temperature dependences of the mean ($\langle\phi_{ester}\rangle$) and variance ($\langle\phi_{ester}^2\rangle - \langle\phi_{ester}\rangle^2$) of the ester dihedral distribution. By symmetry, the first of these does not change with temperature, as is necessarily the case in the conventional RIS treatment. Additional isomeric states of energy E are assigned pairwise on either side of the minimum energy trans state at locations $\pm\delta$, also required by symmetry. The Boltzmann factor-weighted values of $\langle\phi_{ester}\rangle$ and $\langle\phi_{ester}^2\rangle$ were determined for the analytical function (eq 8) over the range of temperatures from 100 to 600 K using

$$\langle\phi_{ester}^{\,n}\rangle = \frac{1}{Z}\int_0^{2\pi}\phi^n \exp(-E_\phi/RT)\,d\phi \tag{9}$$

$$Z = \int_0^{2\pi}\exp(-E_\phi/RT)\,d\phi$$

The behavior of the continuous potential may then be approximated by a series of discrete states symmetric about the minimum energy state at $\phi_{min} = 0°$:

$$\langle\phi_{ester}\rangle = 0°$$

$$\langle\phi_{ester}^{\,n}\rangle = \frac{\sum_i 2\delta_i^{\,n}\exp(-E_i/RT)}{1 + \sum_i 2\exp(-E_i/RT)} \tag{10}$$

By adjustment of i, δ_i, and E_i, the distribution of the ester torsion may be reproduced in the RIS approximation over a wide range of temperatures. As illustrated in Figure 6, a single pair of additional isomeric states having energies

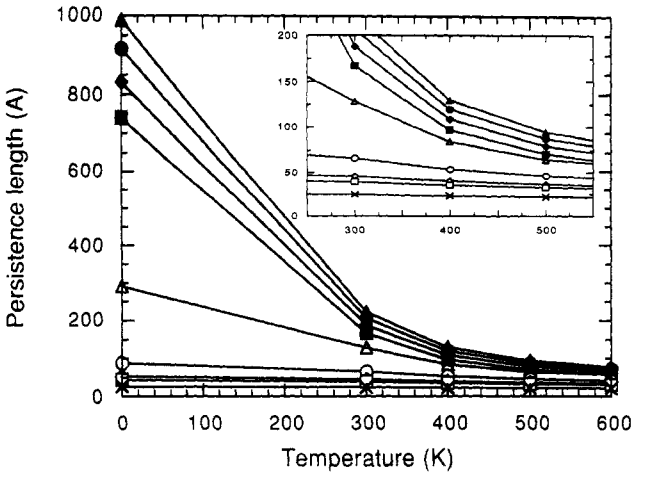

Figure 7. Persistence lengths for various aromatic polyester compositions plotted at 0 K (the conventional RIS method) and over the range of temperatures from 300 to 600 K (from the modified RIS treatment): (▲) PHNA, (●) BN-67, (◆) BN-33, (■) PHBA, (△) HIQ-95, (○) HIQ-74, (◇) HIQ-50, (□) HIQ-34, (×) PPI.

of 1.8 kcal/mol and located at $\delta = \pm 53°$ suffices to emulate fluctuations in the ester torsion within a margin of 3% over the range from 300 to 400 K and within 15% from 250 to 550 K. Increasing the number of states i improves the RIS approximation over a wider range of temperatures. Similar treatment of torsional vibrations about bonds connecting ring groups with neighboring esters would also be feasible, but at considerable cost in wieldiness of the resulting isomeric state matrices; moreover, sensitivity analyses have indicated that this additional complexity would produce relatively little impact on the results.

With the introduction of a three-state ester torsion representation, the RIS calculations were repeated for several BN and HIQ compositions between 0 and 600 K. The temperature dependence of the persistence length for these polyesters is illustrated in Figure 7, with emphasis on the range from 250 to 550 K. These results demonstrate the impact on chain rigidity of torsional fluctuations which populate rotation states on either side of the trans state of the ester dihedral; the effect is most dramatic for those chains which are closest to the rigid rod limit at 0 K. For PHBA, the RIS-predicted value for persistence length drops from 740 to 167 Å at 300 K and 97 Å at 400 K, in reasonable accord with the available experimental data; similarly for BN-67, the calculated persistence length decreases to 188 Å at 300 K and 109 Å at 400 K, compared to the measured value of 120 Å at 333 K. For the HIQ compositions below 75% HBA content, this fall is considerably less dramatic, decreasing from 54 Å at 0 K to 40 Å at 400 K for HIQ-50, and from 44 Å only to 36 Å at 400 K for HIQ-34; these values are well within the range of those determined experimentally.

Indirect Consideration of Packing Forces

Comparison of these results generated by the RIS method for single chains with experimental data from the isotropic melt and solution would suggest that the breadth of the torsion angle distribution is an essential feature for accurate polyarylate simulation. In the solid state, however, the situation should be quite different. Processing methods generally seek to take advantage of the properties of the liquid crystalline phase under elongation flow conditions to induce highly oriented mesophases which are then fixed in place upon cooling the polymer. In this state, the observed distribution of chain conformations may differ quite markedly from that expected in the quiescent solution. These differences may arise due to the external forces exerted by the elongational flow field, which effects are then retained over long periods due to very slow relaxation of the polymer structure in the quenched state, or they may be due to molecular-scale packing forces which serve to stabilize the oriented solid state and possibly lead to crystallization. In either case, the available X-ray diffraction, electron microscopy, and dynamic mechanical observations are consistent with chain conformations that are decidedly elongated in oriented fiber and tape samples. In order to capture this behavior, some expression of these intermolecular or external forces is required. This may be achieved indirectly through another modification of isomeric states and statistical weights. The underlying premise of this approach is that the introduction of neighboring chains and corresponding packing constraints has the *net* effect of favoring certain intramolecular conformations, specifically those which benefit from stabilizing intermolecular interactions, over others which enjoy no such enthalpy of packing.

We treat the presence of neighboring chains nonexplicitly through the introduction of a mean field intermolecular contribution to the potential energy of the system, the dependence of which upon chain conformation may be decoupled from its dependence on other, external parameters. Thus, for the total potential energy of the system described by the chain conformation i as a function of internal conformational degrees of freedom (l, bond length; θ, valence bond angle; ϕ, bond dihedral) and external or intermolecular degrees of freedom (denoted generally as χ), we have

$$E_{\text{total}}\{l,\theta,\phi,\chi\}_i = E_{\text{intramolecular}}\{l,\theta,\phi\}_i + E_{\text{packing}}\{l,\theta,\phi,\chi\}_i \tag{11}$$

Retaining the assumption of constant bond lengths and valence angles and assuming that the external energy contributions due to the degrees of freedom $\{\chi\}_i$ are independent of chain conformation and hence may be decoupled from that portion of the external energy which does depend upon chain conformation, we have

$$E_{\text{total}}\{\phi,\chi\}_i = E_{\text{intramolecular}}\{\phi\}_i + E_{\text{packing}}\{\phi\}_i + E_{\text{packing}}\{\chi\}_i \tag{12}$$

The last term is a constant independent of conformation. The first and second terms on the right-hand side of eq 12 may be combined to define a new effective conformational energy. We assume that the contribution due to $E_{\text{packing}}\{\phi\}_i$ is also primarily short range in nature. This final assumption neglects in effect the influence of long-range ordering forces which operate on the chain as a whole, but it allows extension of the present RIS scheme to the study of chain behavior under constraints imposed by the surrounding medium through the simple redefinition of statistical weights.

This consideration is of greatest interest in the case of the polyesters such as HIQ which contain angular disruptor units; these polymers exhibit thermotropic nematic transitions and melt spinnability despite the strong tendency toward random coil behavior suggested by single-chain calculations and measurements. In this instance we considered first a modified RIS representation which mimics the types of conformations employed by Johnson et al.[19] in their simulation of meridional WAXD from two-dimensional sheets of HIQ-50 and HIQ-33. Their analyses preselected chain conformers of greater extension through limitation of the allowed conformer states available to the

Table VII
Scaling Lengths (Å) for HIQ and HBA/TA/RL Materials under the Imposition of Hypothetical Intermolecular Packing Forces

	PPI	HIQ-50	TA/RL	HBA/TA/RL 25
case I	5.849	5.541	5.045	4.631
case II	6.157	5.963	5.494	5.198

Table VIII
Limiting Values of the Scaled First and Second Moments of the End-to-End Vector and Radius of Gyration of HIQ-50 and the Composition HBA/TA/RL-25 under the Imposition of Hypothetical Intermolecular Packing Forces[a]

	case	$[\lvert\langle \mathbf{r}\rangle\rvert/l^*]_\infty$	C_∞	a (Å)	$[\langle s^2\rangle/nl^{*2}]_\infty$
HIQ-50	I	13.6	30.9	88.4	5.14
	II	39.0	81.7	247	13.5
HBA/TA/RL 25[b]	I	6.55	17.7	43.3	2.95
	II	12.5	28.7	77.2	4.78

[a] Based on calculations for a degree of polymerization of 8193. [b] See text for details of this composition.

monomer units. This entails the following restrictions: (1) The isophthalic acid monomer realizes only the conformation of highest extension, i.e., the conformation in which successive ester bonds are in the syn conformation about the *m*-phenylene ring group. (2) The ester groups flanking the *p*-phenylene moiety of the HQ monomer are coplanar; such planar conformations are either syn or anti in nature, thus halving the number of possible conformers which this monomer may realize. (3) Johnson et al. treated the HBA monomer as planar; this appears to be inappropriate based on the analyses of model compounds described earlier. The correspondence, therefore, between the chains simulated in this section and the "quasi-planar" conformations of Johnson et al. is not exact. Instead, we have allowed all of the original HBA monomer conformations, which may be identified as anti+ (i.e., the ester linkages projected onto the plane of the ring describe a trans state about the imaginary line joining the carbonyl carbon and ester oxygen of the HBA monomer, but the linkage attached to the ester oxygen is rotated out of plane in the positive direction of the right-handed thread), anti−, syn+, and syn−. All other conformation possibilities have been precluded by zeroing the appropriate statistical weights.

For purposes of illustration, we demonstrate two constrained-conformation models for PPI and a representative HIQ composition, HIQ-50. The first of these, designated case I, allows the full set of monomer conformation states described above; the second, designated case II, allows only the anti and anti± conformers of HQ and HBA, respectively. The scaling length varies with changes in the allowed conformations for each monomer; the new values are listed in Table VII for the model cases specified. It may be noted that the PPI case II consists of only a single rodlike conformation, which resembles that adopted by molecules of bis(4-benzoyl-oxyphenyl) isophthalate in the crystal state[44] and is most likely to describe that realized in crystalline PPI. Table VIII illustrates the change in rigidity for HIQ-50 as characterized by $[\lvert\langle \mathbf{r}\rangle\rvert/l^*]_\infty$, C_∞, persistence length a, and $[\langle s^2\rangle/nl^{*2}]_\infty$. Each of the constrained models exhibits greater rigidity than the unconstrained case result listed in Table V, largely due to the elimination of kinked isophthaloyl conformations. Comparison of case I and case II chains illustrates sharply the effect on chain rigidity in HIQ materials of the introduction of syn conformations.

A similar pair of models was applied to the analogous kinked-chain polymer composed of HBA, TA, and RL, whose isolated single-chain behavior is essentially identical to that of HIQ in the conventional RIS treatment. In this instance, case I chains exhibit HBA conformers of anti+ or syn± in kind, while the TA monomer, being planar by nature, may be anti or syn. The RL monomer is constrained to the fully extended syn conformations, by analogy to the constrained IA case, such that ester linkages projected onto the plane of the ring describe a cis orientation about the imaginary bond joining the ester oxygens. In addition, these ester linkages may project either both above the plane of the ring or one above and one below. Case II chains allow only anti and anti± conformations of TA and HBA, respectively. Results for these two models are included in Tables VII and VIII, along with the results for the analogous HIQ types. Comparison of these models reveals the different limiting behaviors, especially under the more severe conformational constraints represented by case II. Although significant increases in apparent stiffness are possible, it must be noted that even the restriction of the RL monomer to its most extended forms is not sufficient to ensure rigidity in HBA/TA/RL of the order observed in the rodlike polymers. The primary distinction between these two types of kinked-chain polymers, then, should lie not in their inherent conformational rigidities, but in the possibility for influence of the conformational rigidity through the introduction of external forces, either intermolecular or imposed extensional in origin.

Conclusions

A wide range of aromatic polyester compositions may be dealt with within a relatively simple, self-consistent rotational isomeric state framework, subject only to the accuracy of parameters derived from quantum mechanics calculations on model compounds. By so doing, the full power of the RIS matrix methods, generalized for constitutional heterogeneity in nonregular polymers by means of analogy to Markov chains, may be brought to bear in the question of compositional variation in aromatic polyesters. In this analysis, we have focused on geometric measures of chain shape and rigidity, parameters of particular interest to this class of materials whose primary applications depend upon their ability to transform into nematic mesophases at elevated temperatures and to retain their highly oriented geometries in processed fibers, tapes, and molded parts. Appropriate scaling of results enables comparison across the full range of polyesters considered. The basic similarities of all of the BN copolymers, encompassing the entire extent of compositions from the pure HBA material to the pure HNA material, are readily apparent in their common characteristic ratios and scaled radius of gyration tensors at equivalent degrees of polymerization. By contrast, the remarkable changes in polymer behavior which accompany compositional variation in the HIQ family of polyesters are realized in the dramatic changes in characteristic ratio and radius of gyration tensor. It is clearly the introduction of angular disruptor units, even in very low quantities, which is the source of these geometric changes, as demonstrated by consideration of various polyesters in which the *m*-phenylene disruptor is introduced via different monomer species.

For comparison of the calculations with experimental data, measures of the characteristic ratio and persistence length in solution or quenched melt provide the closest analogies, although even these measurements are not without their own considerable difficulties. A straightforward modification of the isomeric state assignments

via representation of higher moments of the torsion angle distribution is employed to capture thermal effects on chain conformation; application of this modification to the treatment of the ester linkage suffices to bring the RIS results in line with experimental observations within the present limits of uncertainty.

While this is encouraging from the standpoint of explaining isolated chain behavior in solution, it does not satisfy questions relating to the conformations and orientations of molecular segments in the nematic state or in end-use geometries (e.g., fibers). For this purpose, the conventional RIS approach is more appropriate in the case of rodlike polymers. This relates to the sharper distribution of torsion angles anticipated in the solid state; the large torsional librations observed in solution or in isolated chain calculations are effectively damped out by interactions with neighboring molecules in multichain assemblies. However, even this method overestimates conformational flexibility in the case of the polyarylates with angular disruptor units. In such instances, intermolecular interactions cannot be ignored. A short-range mean field approximation has been considered within the formalism of the isomeric state theory which demonstrates the possible stiffening influence exerted by packing constraints on molecular conformation in multichain assemblies. However, the constraints imposed here were developed essentially a posteriori, being derived from previous efforts to rationalize WAXD observations. It remains to determine the detailed nature of these packing constraints and their interactive dependence on neighbor chain constitutions and conformations.

Acknowledgment. I am grateful to Prof. I. M. Ward for many useful discussions and to the Interdisciplinary Research Centre in Polymer Science and Technology for its much-appreciated support during the course of this work. Financial assistance was provided by the Science and Engineering Research Council by means of a Rolling Grant in Polymer Physics at the University of Leeds.

References and Notes

(1) Geiss, R.; Volksen, W.; Tsay, J.; Economy, J. *J. Polym. Sci., Polym. Lett. Ed.* **1984**, *22*, 433.
(2) Lieser, G. *J. Polym. Sci., Polym. Phys. Ed.* **1983**, *21*, 1611.
(3) Hanna, S.; Windle, A. H. *Polym. Commun.* **1988**, *29*, 236.
(4) Biswas, A.; Blackwell, J. *Macromolecules* **1987**, *20*, 2997.
(5) Biswas, A.; Blackwell, J. *Macromolecules* **1988**, *21*, 3146.
(6) Biswas, A.; Blackwell, J. *Macromolecules* **1988**, *21*, 3152.
(7) Biswas, A.; Blackwell, J. *Macromolecules* **1988**, *21*, 3158.
(8) Troughton, M. J.; Unwin, A. P.; Davies, G. R.; Ward, I. M. *Polymer* **1988**, *29*, 1389.
(9) Troughton, M. J.; Davies, G. R.; Ward, I. M. *Polymer* **1989**, *30*, 58.
(10) Green, D. I.; Unwin, A. P.; Davies, G. R.; Ward, I. M. *Polymer* **1990**, *31*, 579.
(11) Green, D. I.; Davies, G. R.; Ward, I. M. Mechanical modeling of HIQ-35: A novel copolyester with both liquid crystal and crystalline phases. Presented at the meeting of the Polymer Physics Group of the Institute of Physics and The Royal Society of Chemistry, University of Leeds, 9–11 September 1991.
(12) Clements, J.; Humphreys, J.; Ward, I. M. *J. Polym. Sci., Part B: Polym. Phys.* **1986**, *24*, 2293.
(13) Allen, R. A.; Ward, I. M. *Polymer* **1991**, *32*, 2, 202.
(14) Erdemir, A. B.; Johnson, D. J.; Tomka, J. G. *Polymer* **1986**, *27*, 441.
(15) Erdemir, A. B.; Johnson, D. J.; Karacan, I.; Tomka, J. G. *Polymer* **1988**, *29*, 597.
(16) Blundell, D. J.; MacDonald, W. A.; Chivers, R. A. *High Perform. Polym.* **1989**, *1*, 2, 97.
(17) Blundell, D. J.; Chivers, R. A.; Curson, A. D.; Love, J. C.; MacDonald, W. A. *Polymer* **1988**, *29*, 1459.
(18) Johnson, D. J.; Karacan, I.; Tomka, J. G. *J. Text. Inst.* **1990**, *81*, 4, 421.
(19) Johnson, D. J.; Karacan, I.; Tomka, J. G. *Polymer* **1990**, *31*, 8.
(20) Johnson, D. J.; Karacan, I.; Tomka, J. G. *Polymer* **1992**, *33*, 983.
(21) Rutledge, G. C.; Ward, I. M., submitted to *J. Polym. Sci., Part B: Polym. Phys.*
(22) Flory, P. J. *Statistical Mechanics of Chain Molecules*; Hansen Publishers: Munich, 1988.
(23) Flory, P. J. *Macromolecules* **1974**, *7*, 381.
(24) Flory, P. J.; Yoon, D. Y. *J. Chem. Phys.* **1974**, *61*, 5358.
(25) Coulter, P.; Windle, A. H. *Macromolecules* **1989**, *22*, 1129.
(26) Lautenschläger, P.; Brickmann, J.; van Ruiten, J.; Meier, R. J. *Macromolecules* **1991**, *24*, 1284.
(27) Use of the matrices presented in ref 23 in the calculation of properties for chains with independent rotation potentials requires a slight modification of the equations presented earlier in ref 22. In particular, the change in organization of the elements of G_i (eq IV-24, ref 22) to those of F_i (eq 45, ref 23) lead to the following substitution for eq IV-69 of ref 22: $\mathbf{F}_i^{(\xi)} = [\mathrm{col}(1,1,1...1) \otimes E_s]\mathbf{F}_i^{(\xi)*}$, $\mathbf{E}_s$ being the identity matrix of order s required by the generator matrix $\mathbf{F}_i$ (e.g., $s = 5$ for $\langle r^2 \rangle$ calculations), and the length of the column vector corresponds to the number of isomeric states ν.
(28) Hummel, J. P.; Flory, P. J. *Macromolecules* **1980**, *13*, 479.
(29) Available through the Department of Chemistry, Indiana University, Bloomington, IN 47405: *QCPE No. 455*, 1990.
(30) Available through Gaussian, Inc., 4415 Fifth Ave., Pittsburgh, PA 15213.
(31) Marriott, S.; Silvestro, A.; Topsom, R. D. *J. Chem. Soc., Perkin Trans. 2* **1988**, 457.
(32) Williams, A. D.; Flory, P. J. *J. Polym. Sci., Part A-2* **1967**, *5*, 417.
(33) Erman, B.; Flory, P. J.; Hummel, J. P. *Macromolecules* **1980**, *13*, 484.
(34) Theodorou, D. N.; Suter, U. W. *Macromolecules* **1985**, *18*, 1206.
(35) Šolc, K. *J. Chem. Phys.* **1971**, *55*, 335.
(36) It may be noted that any minor differences observed by Erman et al.[33] between type I and type II polymers is a result of their method of scaling the type II material. In the type I material there is only a single monomer type, and no ambiguity is introduced by taking it as the first monomer in the chain. For the type II material, where two monomer types are involved, these authors assume the identity of the first monomer and scale accordingly; eq 2 weights appropriately the equal possibilities for either monomer to initiate the chain. In the absence of coupling effects, the scaling lengths for type I and type II polymers are identical and the overlap of curves is exact.
(37) Tsvetkov, V. N.; Andreeva, L. N.; Lavrenko, P. N.; Okatova, O. V.; Beliaeva, E. V.; Bilibin, A. Yu.; Skorokhodov, S. S. *Eur. Polym. J.* **1985**, *21*, 933.
(38) Tsvetkov, V. N.; Andreeva, L. N.; Bushin, S. V.; Belyayeva, Ye. V.; Cherkasov, V. A.; Mashoshin, A. I.; Bilibin, A. Yu.; Skorokhodov, S. S. *Vysokomol. Soedin.* **1988**, *A30*, 713.
(39) Krigbaum, W. R.; Tanaka, T. *Macromolecules* **1988**, *21*, 743.
(40) Krömer, H.; Kuhn, R.; Pielartzik, H.; Siebke, W.; Eckhardt, V.; Schmidt, M. *Macromolecules* **1991**, *24*, 1950.
(41) MacDonald, W. A.; McLenaghan, A. D. W.; Richards, R. W. *Polymer* **1990**, *31*, 684.
(42) MacDonald, W. A.; McLenaghan, A. D. W.; Richards, R. W. *Macromolecules* **1992**, *25*, 826.
(43) Jung, B.; Schürmann, B. L. *Macromolecules* **1989**, *22*, 477.
(44) O'Mahoney, C. A.; Williams, D. J.; Colquhoun, H. M.; Blundell, D. J. *Polymer* **1990**, *31*, 1603.

Registry No. TA, 100-21-0; HBA, 99-96-7; HQ, 123-31-9; IP, 121-91-5; mBA, 99-06-9; RL, 108-46-3; BP, 58574-03-1; HNA, 16712-64-4; ND, 581-43-1; PHNA (homopolymer), 94857-18-8; PHNA (SRU), 87257-45-2; BN-33, 81843-52-9; PHBA (homopolymer), 30729-36-3; PHBA (SRU), 26099-71-8; PPT (copolymer), 26618-60-0; PPT (SRU), 26637-45-6; HIQ-99, 31072-57-8; PPI (copolymer), 26809-66-5; PPI (SRU), 26857-09-0; (HBA)(TA)(ND) (copolymer), 78390-26-8; (HBA)(TA)(BP)(HNA) (copolymer), 122122-87-6; (HBA)(TA)(RL) (copolymer), 31072-55-6; (TA)(RL) (copolymer), 29660-01-3; (TA)(RL) (SRU), 32037-95-9; (mHBA)(TA)(HQ) (copolymer), 141613-78-7; (HBA)(mHBA) (copolymer), 80181-33-5; (HBA)(mHBA) (SRU), 55069-85-7; $HO_2C(C_6H_4\text{-}p\text{-})_2CO_2H$, 787-70-2; $HO(C_6H_4\text{-}p\text{-})_2OH$, 92-88-6; 2,6-dinaphthoic acid, 1141-38-4; phenyl benzoate, 93-99-2.